Photolysis of iron(III)-carboxylato complexes – Quantum yield determination and reactivity simulation in clouds and atmospheric particles

C. Weller, A. Tilgner, P. Bräuer, H. Herrmann

Atmospheric Chemistry Department (ACD), Leibniz Institute for Tropospheric Research (TROPOS), Leipzig, Germany

contact: christian.weller@tropos.de

Motivation and Background

Iron-complex photochemistry in the atmospheric aqueous phase

Iron is always present in concentrations from ~10^{-9} (clouds) up to ~10^{-3} M (fog, particles). Iron sources are mainly mineral dust emissions. Iron complexes are very good absorbers in the UV-VIS actinic region and photo-chemically reactive through LMCT (ligand to metal charge transfer) transitions. Fe-complex photolysis leads to radical production (see Fig. 1). The photochemistry initiates radical chain reactions, which is related to the oxidizing capacity of the troposphere and promotes ligand decomposition. The Fe^{2+} budget is important for the Fenton-reaction, which can be a considerable in-situ OH source in the aqueous phase.

Fig. 1: Photolysis of Fe(III)-oxalato complex as example, including subsequent reactions.

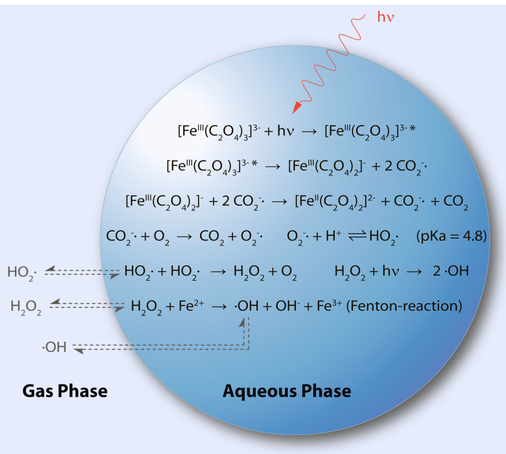

Measurement of overall Fe^{2+} quantum yield

- De-oxygenation with Argon-bubbling prior to photolysis, if desired
- Direct photolysis in quartz-cuvette:

Fig. 2: Experimental setup for complex photolysis with excimer laser (20ns pulse) or HgXe-lamp (continuous irradiation).

- Measurement of Excimer laser energy with calibrated pyro-electric sensor
- Ferrioxalate actinometry to determine HgXe-lamp photon flux (Hatchard and Parker, 1956)
- Measurement of Fe^{2+} as $[Fe(Phen)_3]^{2+}$, $e_{l\,=\,510\,nm}$ = 11 100 $M^{-1}cm^{-1}$ UV-VIS spectrometer
- Calculation of iron speciation with speciation program (Species, Visual Minteq)

Results and Discussion

Table 1: Measured quantum yields after flash photolysis, primary and secondary photo-reaction steps as well as observed effects of dissolved O_2 and increased excitation energy (E↑) on Fe^{2+} quantum yield, F↓ stands for Fe^{2+} quantum yield decrease, F↑ for increase, n.d. is not determined.

Ligand/ Complex	Ar/ O_2	308 nm	351 nm	O_2 effect 308 nm	O_2 effect 351 nm	E↑ effect 308 nm	E↑ effect 351 nm
Oxalate	Ar	not determined due to experimental limitations		n.d.	n.d.	O_2 n.d. Ar Φ↓	n.d.
*$[Fe(OOCCOO)_2]^-$ *$[Fe(OOCCOO)_3]^{3-}$	Ar	0.93±0.09	0.88±0.08	Φ↓	Φ↓		
Malonate #$[Fe(CH_2(COO)_2)_2]^-$	O_2	0.024±0.001	0.040±0.003	n.d.	n.d.	n.d.	n.d.
Tartronate #$[Fe(OOCCHOHCOO)_2]^-$	O_2	0.79±0.02	0.78±0.06	Φ↓	Φ↓	O_2 Φ↓ Ar Φ↓	O_2 no eff Ar Φ↓
	Ar	0.90±0.02	1.10±0.08				
Succinate #$[Fe((CH_2)_2(COO)_2)_2]^-$	O_2	0.24±0.02	0.17±0.005	no effect	Φ↑	O_2 Φ↓ Ar Φ↓	O_2 no eff Ar no eff
	Ar	0.23±0.02	0.12±0.01				
Tartrate #$[Fe((CHOH)_2(COO)_2)]^+$	O_2	0.57±0.07	0.57±0.02	no effect	no effect	n.d.	n.d.
	Ar	0.56±0.07	0.55±0.02				
#$[Fe((CHOH)_2(COO)_2)_2]^-$	O_2	0.61±0.08	0.76±0.05	no effect	no effect	O_2 n.d. Ar no eff	O_2 n.d. Ar no eff
	Ar	0.63±0.09	0.76±0.02				
Glutarate $[Fe((CH_2)_3(COO)_2)]^-$	O_2	0.021±0.001	0.017±0.002	n.d.	n.d.	n.d.	n.d.
Pyruvate #$[FeOOCCOCH_3]^{2+}$	O_2	0.47±0.07	0.64±0.02	Φ↓	Φ↓	n.d.	n.d.
	Ar	0.63±0.07	0.76±0.07				
Glyoxalate #$[Fe(OOCC(OH)_2)]^{2+}$	O_2	0.76±0.05	0.77±0.06	Φ↓	Φ↓	O_2 Φ↓ Ar Φ↓	O_2 n.d. Ar Φ↓
	Ar	1.21±0.05	1.06±0.02				
Gluconate $[Fe(HOCH_2(CHOH)_4$ $-COO)_2(OH)_3]^{2-}$	O_2	0.04±0.01	0.03±0.01	n.d.	n.d.	n.d.	n.d.
	Ar	0.05±0.01	0.05±0.01				

*Species already in "Ref wo"; #Species new included in "Ext Fe"

- The quantum yields can differ up to one order of magnitude among different ligands (Tab.1, Fig.3)
- In most cases $F_{argon} > F_{oxygen}$ → indicates the dependence of most F on secondary reactions involving produced radicals with oxygen and subsequent reactions
- Fe(III)-complexes with oxalate, tartronate, succinate and glyoxalate show decreasing quantum yields with an increasing amount of absorbed photons, when the incident laser-energy was increased, most likely due to a change of concentration ratios ratio of secondarily produced radicals towards non-photolyzed complexes

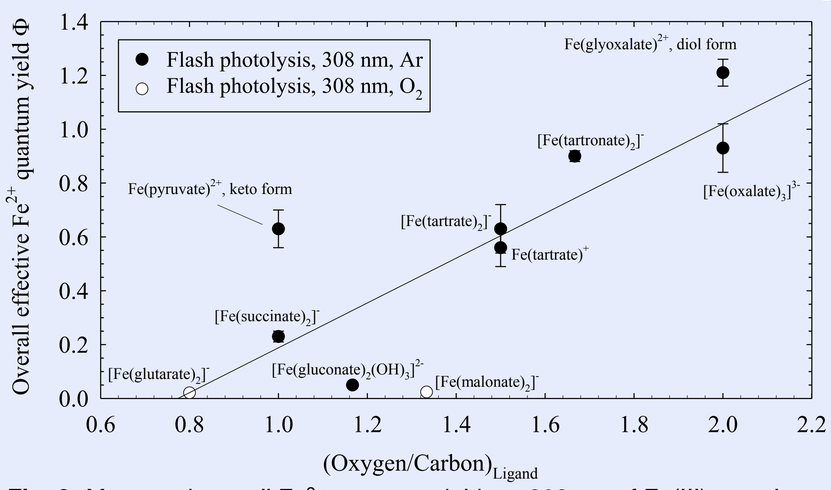

Fig. 3: Measured overall Fe^{2+} quantum yields at 308 nm of Fe(III) complexes investigated in this work as function of oxygen to carbon ratio of the ligand.

- Higher quantum yields of Fe(III) complexes with ligands that have a higher oxygen to carbon ratio (glyoxalate, oxalate) (Fig.1)
- Oxygen can be present in three different substituents in the carboxylates considered in this work, the carboxylate, hydroxy and keto-group. Additionally, the keto-form can be hydrated, forming a gem-diol
- Oxygen substitution is thought to affect the photoreactivity in two ways:

(i) Via inductive effects causing better LMCT in the primary reaction step

(ii) Oxygen influence can also occur via the presence of an oxygen containing group on the C-atom next to the LMCT-involved carboxylate group which enables a two electron oxidation product of the ligand → further Fe(II) can be produced

- Peroxyl radicals formed from ligand fragments of tartronate, tartrate and glyoxalate can undergo an HO_2 elimination which can further cause secondary Fe^{2+} production
- The individual extinction coefficients are similar to those measured by Faust and Zepp (1993)
- The individual quantum yield F_i of $[FeOx_2]^-$ is higher than that of $[FeOx_3]^{3-}$ in both studies, Faust and Zepp (1993) measured lower quantum yields due to use of a lower $[Fe(III)]_{initial}$ than in this study

Individual quantum yields of $[Fe(Ox)_2]^-$ and $[Fe(Ox)_3]^{3-}$ complexes

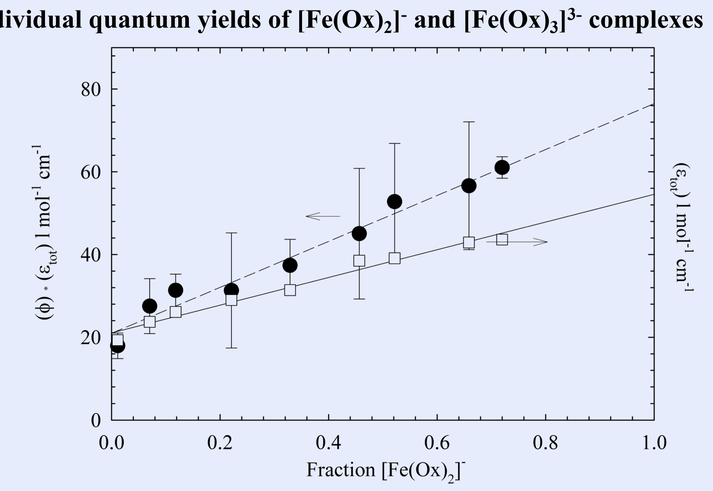

Fig. 4: Product of overall quantum yields (F) and overall extinction coefficients (e_{total}) of $[FeOx_2]^-$ and $[FeOx_3]^{3-}$ mixtures as a function of calculated fraction $[FeOx_2]^-$, HgXe-lamp photolysis @ 436 nm, Ar purged, I = 0.01 M, $[Fe(III)]_{total} = 4.85 \cdot 10^{-4}$ M.

- The sum of both $[FeOx_2]^-$ and $[FeOx_3]^{3-}$ contained always 100% of the total Fe(III)
- Individual extinction coefficients e_i and individual quantum yields F_i of $[FeOx_2]^-$ and $[FeOx_3]^{3-}$ complexes were determined at 436 nm (Tab.2) from the intercepts of the regression lines (Fig.4)

Table 2: Individual quantum yields of Fe(III) 1:2 and 1:3 oxalato complexes obtained from continuous Hg(Xe)-lamp photolysis at 436 nm.

436 nm	$[Fe(Ox)_2]^-$	$[Fe(Ox)_3]^{3-}$	Ref.
ε_i [l mol^{-1} cm^{-1}]	55 ± 9	22 ± 2	this work
ε_i [l mol^{-1} cm^{-1}]	62 ± 6	24 ± 4	[*Faust and Zepp*, 1993]
Φ_i	1.4 ± 0.4	1.0 ± 0.2	this work
Φ_i	1.0 ± 0.25	0.60 ± 0.46	[*Faust and Zepp*, 1993]

Aqueous-phase chemistry modeling

Relevant Fe(III) complex photolysis reactions of species from Tab. 1 were implemented in CAPRAM (Chemical Aqueous Phase Radical Mechanism) as "extended Fe-carboxylate photochemistry" (Ext Fe). Former version of CAPRAM contained only Fe-sulfato, Fe-hydroxy and Fe-oxalato complex photochemistry (Ref wo, Tilgner and Herrmann, 2010). CAPRAM as part of the SPectral Aerosol Cloud Chemistry Interaction Model (SPACCIM; Wolke et al., 2005) has been applied in a 4.5 day non-permanent cloud simulation including 8 cloud passages between deliquescent particle periods.

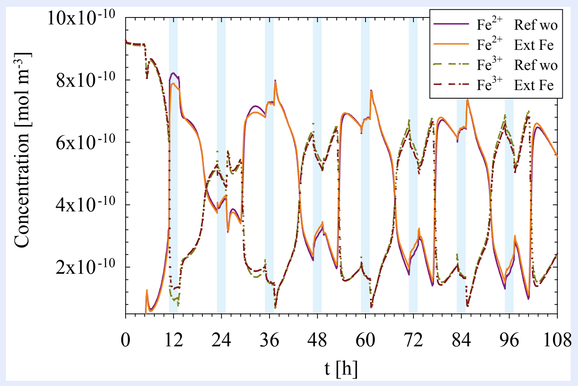

Fig. 6: Simulated concentrations of Fe^{2+} and Fe^{3+} as sum of all species for the respective oxidation state in both "Ref wo" and "Ext Fe" runs.

Fe(III) complex photolysis as important carboxylate sink

The inclusion of the photolysis of malonate, tartronate, succinate, tartrate and glyoxalate Fe-complexes had only minor effect on their degradation (Tab. 4), whereas the complex photolysis contributed with 40% to the depletion of pyruvate (also pyruvic acid included) (see Fig. 5). For oxalate, tartronate and tartrate, the Fe-complex photolysis is also a major sink.

Fe(III) carboxylate photolysis as a radical source?

All newly included carboxylates contribute into peroxyl radical reaction channels through their Fe-complex photolysis from which HO_2 radical is formed. However, their overall contribution to the total HO_2 sources remains small (together 1.3%, Tab. 3) with respect to peroxyl radical reaction channels that originate from other radical reactions like OH, NO_3 and SO_4^-. Uptake of HO_2 from the gas phase is the most important source for the aqueous phase.

Table 3: Contributions of peroxyl radicals $RO_2\cdot$ or $CO_2^{-}\cdot$ from Fe(III) complex photolysis or radical reactions to total simulated daytime $HO_2\cdot/O_2^{-}\cdot$ source fluxes.

$RO_2\cdot/CO_2^{-}\cdot$	Contribution $RO_2\cdot/CO_2^{-}\cdot$ decay to daytime $HO_2\cdot/O_2^{-}\cdot$ [%]	Contribution FeL + hν to daytime $RO_2\cdot/CO_2^{-}\cdot$ [%]	Contribution FeL + hν to daytime $HO_2\cdot/O_2^{-}\cdot$ [%]	Fe(III) complex with
$\cdot CO_2^-$	1.2	96.3	1.1	Oxalate
$\cdot O_2CH(OH)_2$	4.3	0.70	0.03	Glyoxalate
$CH_3C(OH)_2O_2\cdot$	33.0	0.39	0.13	Pyruvate
$\cdot O_2CH(OH)COO^-$	0.07	2.3	0.002	Tartronate
$\cdot O_2CH(OH)CH(OH)COO^-$	0.02	100.0	0.02	Tartrate

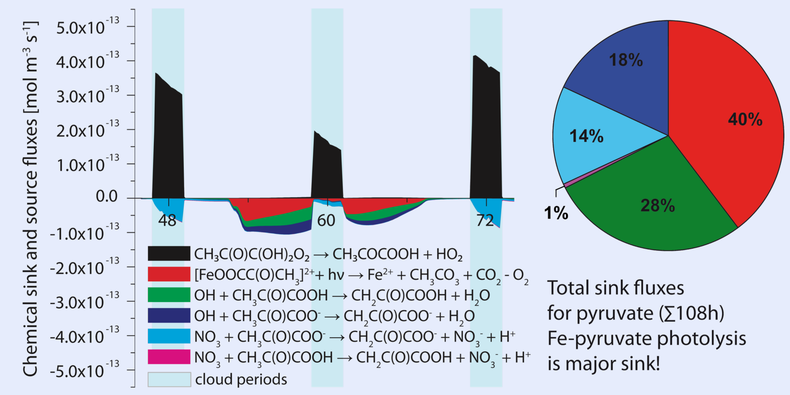

Total sink fluxes for pyruvate (Σ108h) Fe-pyruvate photolysis is major sink!

Figure 5: Major sink and source fluxes for pyruvate in the model run with extended Fe-photochemistry.

Table 4: Fraction of main sink reactions of the ligands (L) with respect to sum the of all sink reactions for total simulation (∑108h).

Sink reaction	Pyruvate [%]	Glyoxalate [%]	Malonate [%]	Oxalate [%]	Succinate [%]	Tartronate [%]	Tartrate [%]
FeL + hν	**39.7**	**2.3**	-	-	**3.5**	-	**91.2**
FeL_2 + hν	-	-	**5.6**	**98.2**	**0.4**	**46.4**	**8.8**
FeL_3 + hν	-	-	-	**0.7**	-	-	-
$LH/LH_2 + \cdot OH$	27.7	93.3	20.9	< 0.05	87.7	29.0	-
$L^-/LH^- + \cdot OH$	18.0	3.9	73.2	0.6	7.7	24.2	-
$LH/LH_2 + NO_3\cdot$	0.8	0.1	0.1	< 0.05	0.1	0.2	-
$L^-/LH^- + NO_3\cdot$	13.8	< 0.05	0.2	0.4	0.6	0.1	-
$LH/LH_2 + SO_4^{-}\cdot$	-	0.5	-	-	-	-	-

Conclusions

- Most investigated Fe-complex photolysis processes involve secondary reactions that influence their experimentally determine quantum yields
- Quantum yields depend on experimental parameters (oxygen saturation, incident energy) and structure of different ligands
- Fe(III)-complex photolysis represents a major sink for some carboxylates in the atmosphere besides radical reactions
- Inclusion of new Fe(III)-carboxylate photochemical reactions in CAPRAM
- SPACCIM model did not significantly affect the Fe(II) budget (Fig.6)
- No significant contribution to radical formation

References: Faust & Zepp (1993) *Environ. Sci. Technol.*, 27, 2517-2522; Hatchard & Parker (1956) *Proc. R. Soc. Lond., Ser. A,* 235, 518; Tilgner and Herrmann (2010) *Atmos. Environ.,* 44 (40), 5415-5422; Wolke (2005) Atmos. Environ., 39 (23-24), 4375-4388